Electronic Supplementary Material (ESI) for Dalton Transactions.

Supplementary Information

Aryl C-O Oxidative Addition of Phenol Derivatives to Nickel Supported by an N-Heterocyclic Carbene via a Ni^0 Five-Centered Complex

Chayapat Uthayopas [a] *and Panida Surawatanawong** [a,b]

[a]Department of Chemistry and Center of Excellence for Innovation in Chemistry, Faculty of Science, Mahidol University, Bangkok 10400, Thailand.

[b]Center of Sustainable Energy and Green Materials, Mahidol University, Salaya, Nakhon Pathom 73170, Thailand

Table S1 Relative free energies (in kcal/mol) with respect to NiL_2 (L = SIPr) for aryl C-O

	IN1_3	**TS_3**
B3LYP/BS1	9.6	28.4
CPCM-B3LYP/BS1	8.9	27.0
CPCM-M06/BS2//B3LYP/BS1	8.1	37.1
CPCM-M06/BS2//CPCM-B3LYP/BS1	7.7	36.2
wB97XD/BS1	18.9	45.1
M06L/BS1	14.9	41.7

oxidative addition of Naph-OMe via three-centered transition states.

Table S2 Relative free energies (in kcal/mol) with respect to NiL_2 (L = SIPr) for aryl C-O

	IN1_3_LA	**TS_3_LA**	**IN1_5_LA**	**TS_5_LA**
B3LYP/BS1	-3.7	20.6	1.6	15.4
CPCM-B3LYP/BS1	-4.3	20.2	2.2	14.9
CPCM-M06/BS2//B3LYP/BS1	2.1	31.1	12.2	30.9
CPCM-M06/BS2//CPCM-B3LYP/BS1	1.8	31.8	11.1	30.6
wB97XD/BS1	-7.4	20.3	-5.4	16.9
M06L/BS1	-4.1	17.4	-4.0	16.7

oxidative addition of Naph-OMe with assistance of Lewis acid (LA = $AlMe_3$) via three- and five-centered transition states.

Distortion-interaction analysis

The distortion-interaction model[1-7] can be used to provide insights into the difference in the energy barriers. The transition state **TS_3** (or **TS_5**) structure, which is obtained from gas-phase optimization using B3LYP/BS1, was separated into two distorted fragments: Ni-SIPr catalyst and ArOR[1] substrate. The single-point energy calculations using M06/BS2 in gas-phase were performed on these two fragments. The distortion energy was calculated from the difference between the electronic energies of the distorted fragment structure and the optimized structure of the Ni-SIPr catalyst ($\Delta E_{dist\text{-}cat}$) or the ArOR[1] substrate ($\Delta E_{dist\text{-}sub}$). While the relative energy (ΔE_{rel}) is the electronic energy of the transition state relative to that of the optimized Ni-SIPr and ArOR[1] fragments, the interaction energy (ΔE_{int}) was calculated from

the difference between the relative energy (ΔE_{rel}) and the total distortion energy ($\Delta E_{dist\text{-}cat} + \Delta E_{dist\text{-}sub}$).

Table S3 Distortion/interaction decomposition analysis, NBO charge (q), and C_{Ar}-O bond distance of **TS_3** for aryl C-O OA of ArOX.

Ar-OX	distortion/interaction analysis (kcal/mol)				NBO charge			C_{Ar}-O bond distance (Å)	
	ΔE_{rel}	$\Delta E_{dist-cat}$	$\Delta E_{dist-sub}$	ΔE_{int}	q_{Ni}	q_{Ar}	q_{OX}	TS	free substrate
Ar-OR[1]									
Ph-OMe	-8.3	3.7	42.2	-54.2	0.286	-0.084	-0.331	1.673	1.368
Naph-OMe	-11.6	3.9	41.8	-57.3	0.302	-0.117	-0.328	1.675	1.369
Ph-OPh	-13.1	3.9	29.5	-46.5	0.237	-0.002	-0.356	1.610	1.383
Ph-OC(O)R[2]									
Ph-OC(O)NEt_2	-13.3	2.9	22.4	-38.6	0.188	0.070	-0.360	1.565	1.394
Ph-OC(O)NH_2	-11.3	2.8	22.2	-36.3	0.183	0.082	-0.369	1.569	1.397
Ph-OC(O)^{t}Bu	-13.3	3.2	21.4	-37.8	0.183	0.086	-0.375	1.566	1.399
Ph-OC(O)Me	-11.7	2.9	23.4	-38.0	0.195	0.078	-0.383	1.590	1.401
Ph-OC(O)Ph	-12.5	3.0	22.1	-37.5	0.195	0.095	-0.399	1.572	1.399
Ph-OS(O)$_2$R[3]									
Ph-OS(O)$_2NMe_2$	-18.4	3.6	23.0	-45.0	0.200	0.081	-0.394	1.586	1.405
Ph-OS(O)$_2$Me	-16.3	3.1	20.8	-40.1	0.180	0.091	-0.393	1.572	1.407
Ph-OS(O)$_2$(*p*-Tol)	-16.7	3.1	21.1	-40.9	0.196	0.083	-0.395	1.567	1.405
Ph-OS(O)$_2CF_3$	-17.1	2.5	13.8	-33.5	0.127	0.158	-0.411	1.524	1.417

Table S4 Distortion/interaction decomposition analysis, NBO charge (q), and C_{Ar}-O bond distance of **TS_5** for aryl C-O OA of PhOX.

Ar-OX	distortion/interaction analysis (kcal/mol)				NBO charge			C_{Ar}-O bond distance (Å)	
	ΔE_{rel}	$\Delta E_{dist-cat}$	$\Delta E_{dist-sub}$	ΔE_{int}	q_{Ni}	q_{Ar}	q_{OX}	TS	free substrate
Ph-OC(O)R[2]									
Ph-OC(O)^{t}Bu	-21.4	8.3	58.2	-87.9	0.571	-0.160	-0.490	1.870	1.399
Ph-OC(O)Me	-21.2	7.6	56.8	-85.7	0.569	-0.160	-0.488	1.862	1.401
Ph-OC(O)Ph	-22.3	7.8	55.6	-85.7	0.560	-0.159	-0.493	1.839	1.399
Ph-OS(O)$_2$R[3]									
Ph-OS(O)$_2$Me	-21.9	9.1	50.7	-81.7	0.538	-0.113	-0.516	1.767	1.407
Ph-OS(O)$_2$(*p*-Tol)	-25.1	8.2	52.5	-85.8	0.547	-0.112	-0.537	1.793	1.405
Ph-OS(O)$_2CF_3$	-28.8	8.9	38.1	-75.8	0.490	-0.081	-0.508	1.700	1.417

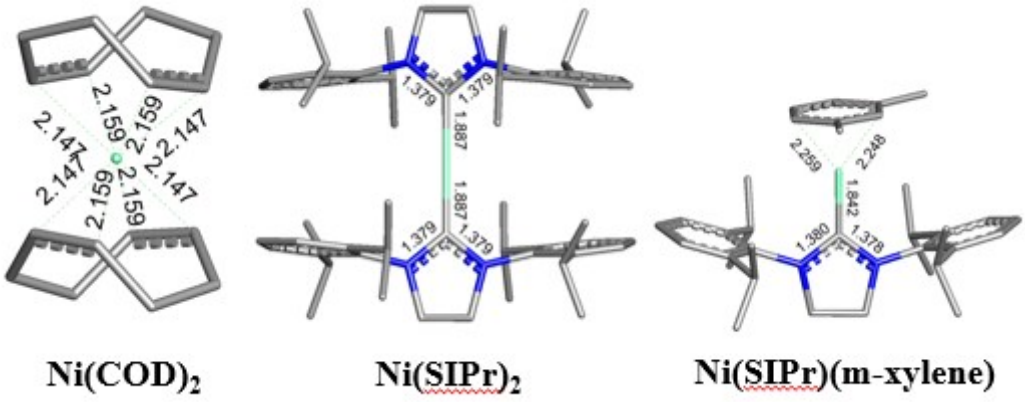

Fig. S1 Optimized structures of $Ni(COD)_2$, $Ni(SIPr)_2$, and Ni(SIPr)(*m*-xylene). Hydrogen atoms are omitted for clarity. Bond distances are shown in Å.

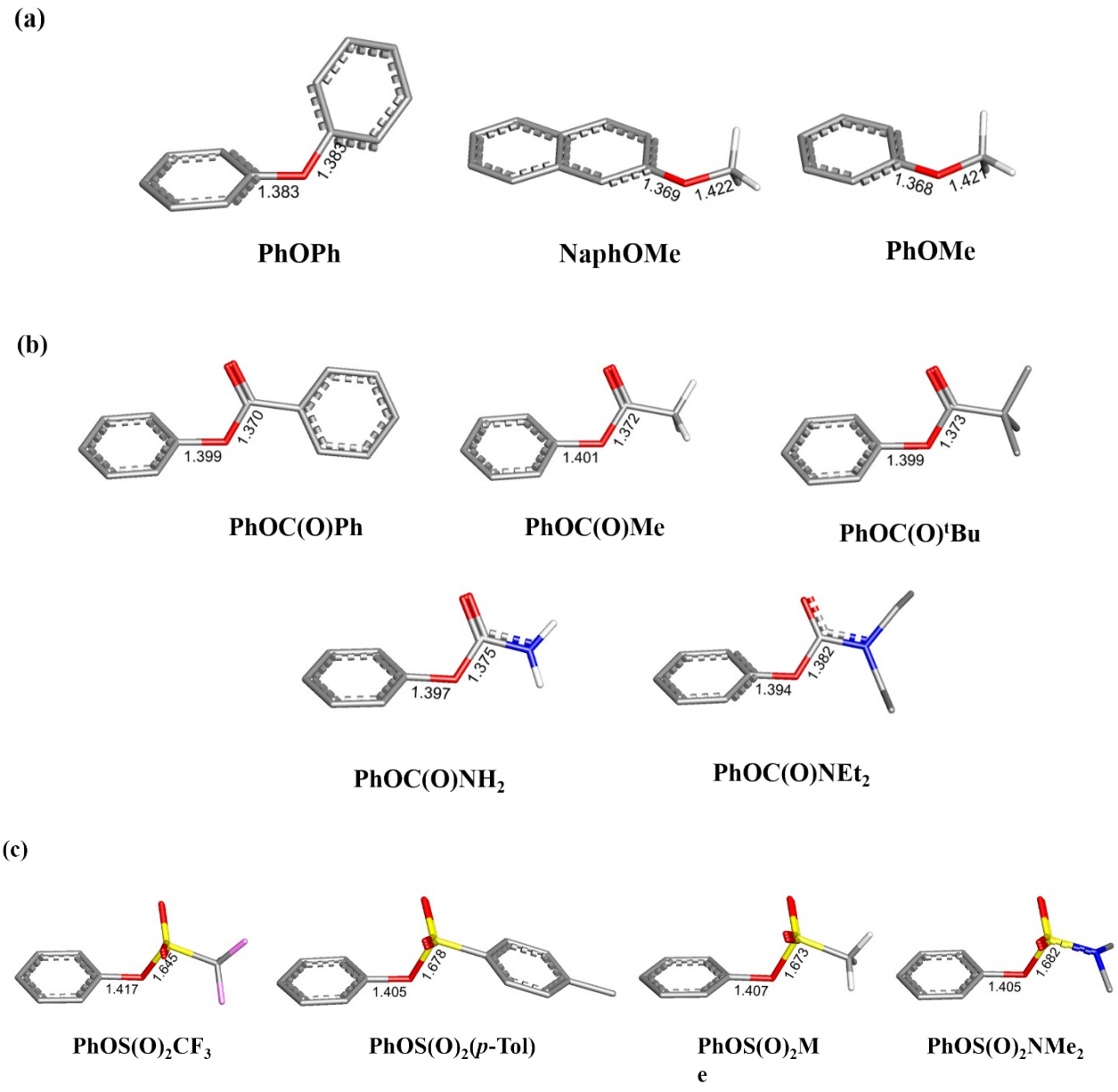

Fig. S2 Optimized structures of (a) aryl ethers, $ArOR^1$: PhOPh, NaphOMe, and PhOMe, (b) phenyl esters/carbamates: $PhOC(O)R^2$ (R^2 = Ph, Me, ^{t}Bu, NH_2, and NEt_2), and (c) phenyl sulfonates/sulfamate: $PhOS(O)_2R^3$ (R^3 = CF_3, *p*-Tol, Me, and NMe_2). Hydrogen atoms are omitted for clarity except for those on OMe and NH_2. Bond distances are shown in Å.

PhOMe

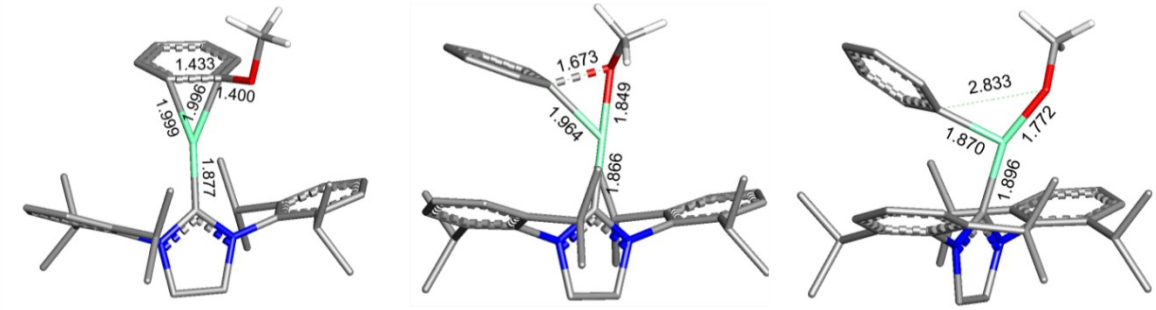

IN1_3 **TS_3** **IN2_3**

NaphOMe

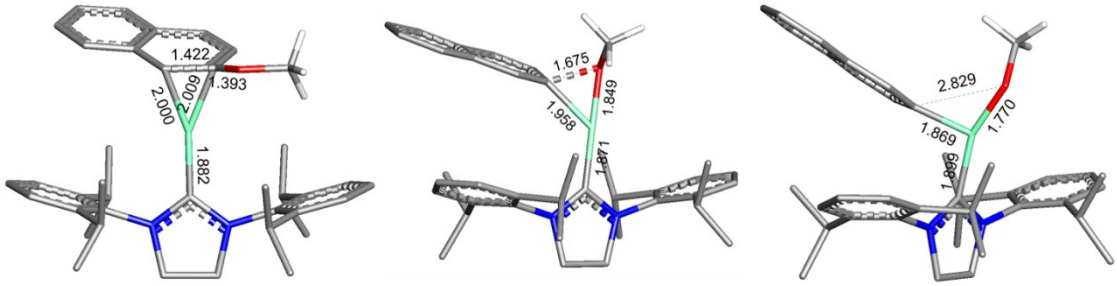

IN1_3 **TS_3** **IN2_3**

PhOPh

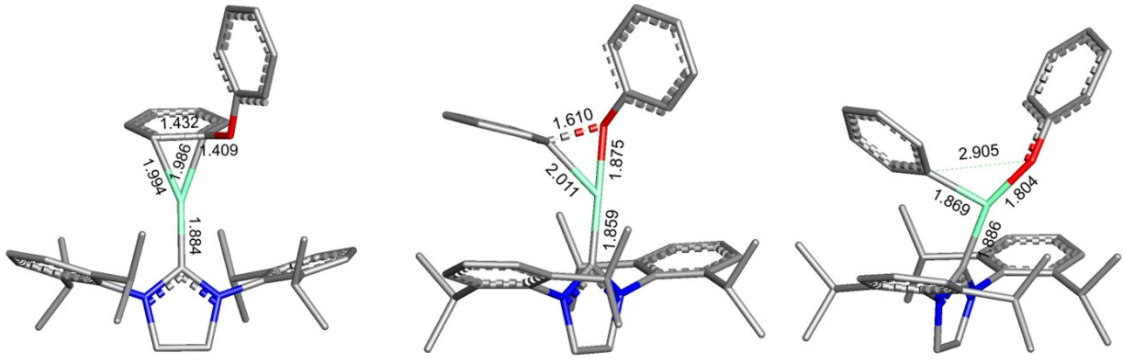

IN1_3 **TS_3** **IN2_3**

Fig. S3 Optimized structures of **IN1_3**, **TS_3**, and **IN2_3** for aryl C-O oxidative addition of aryl ethers, ArOR[1]: PhOMe, NaphOMe, and PhOPh. Hydrogen atoms are omitted for clarity except for those on OMe. Bond distances are shown in Å.

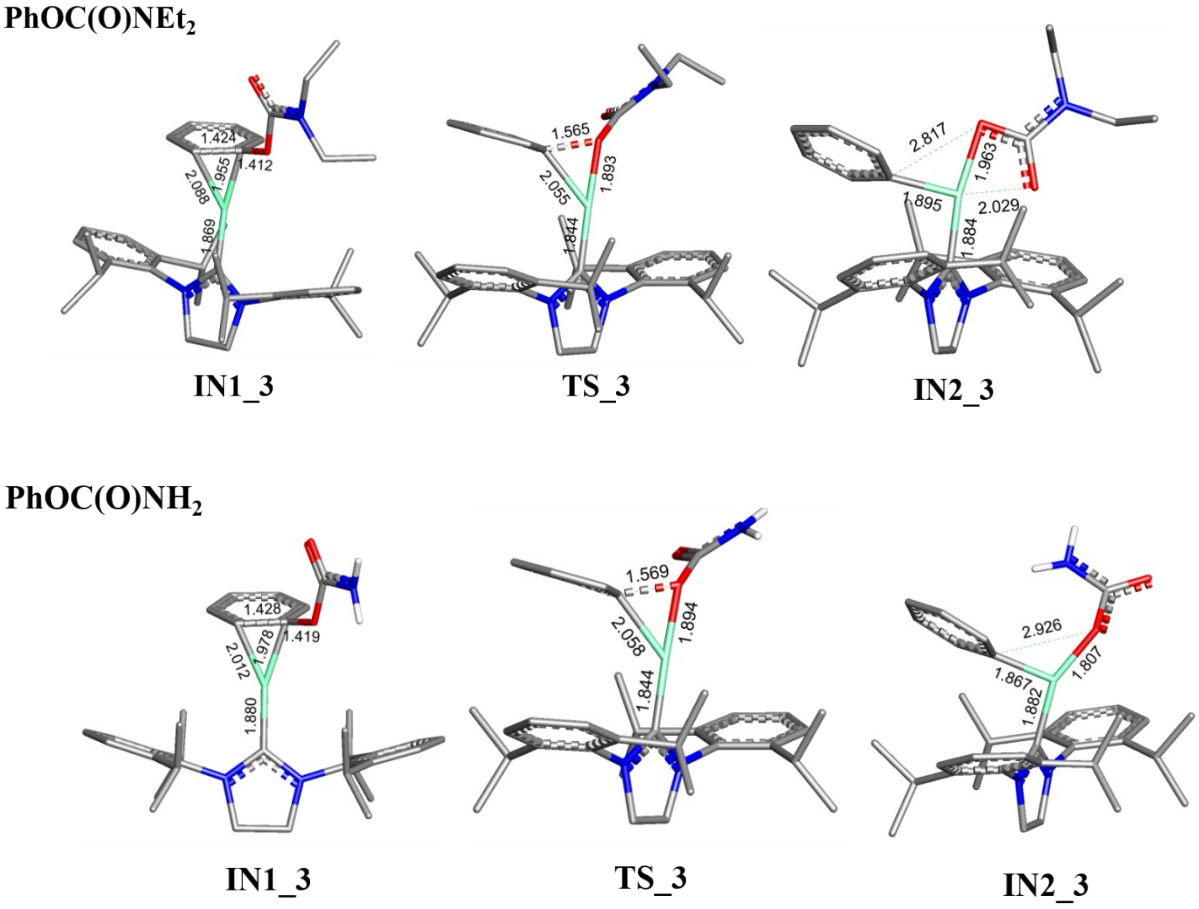

Fig. S4 Optimized structures of **IN1_3**, **TS_3**, and **IN2_3** for aryl C-O oxidative addition of phenyl carbamates: PhOC(O)R^2 (R^2 = NEt_2, and NH_2). Hydrogen atoms are omitted for clarity except for those on NH_2. Bond distances are shown in Å.

PhOC(O)^{t}Bu

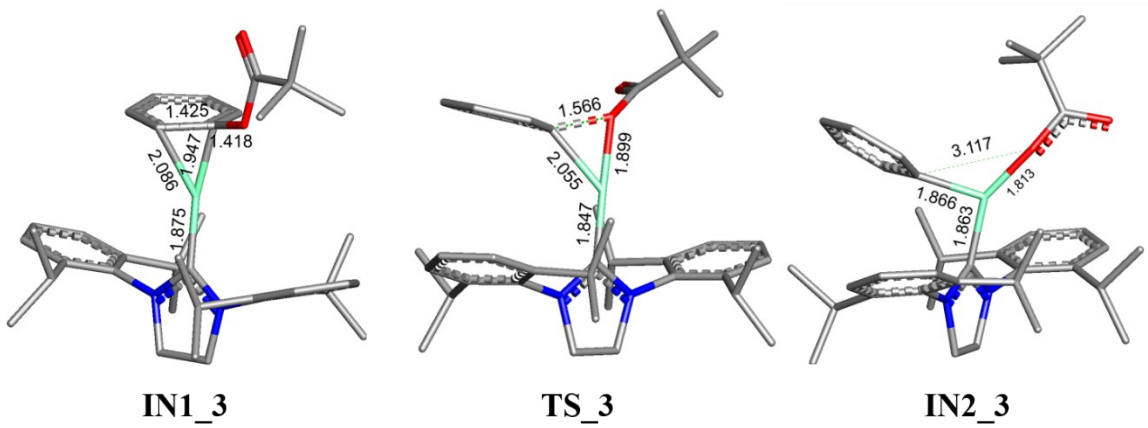

IN1_3 **TS_3** **IN2_3**

PhOC(O)Me

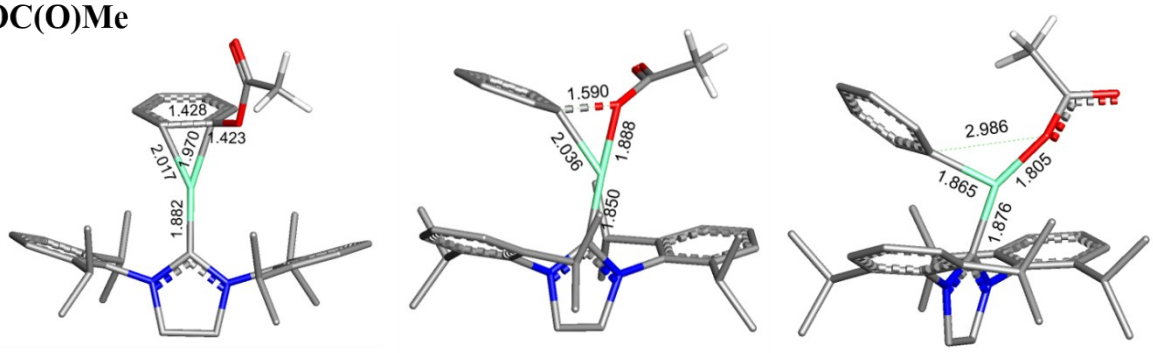

IN1_3 **TS_3** **IN2_3**

PhOC(O)Ph

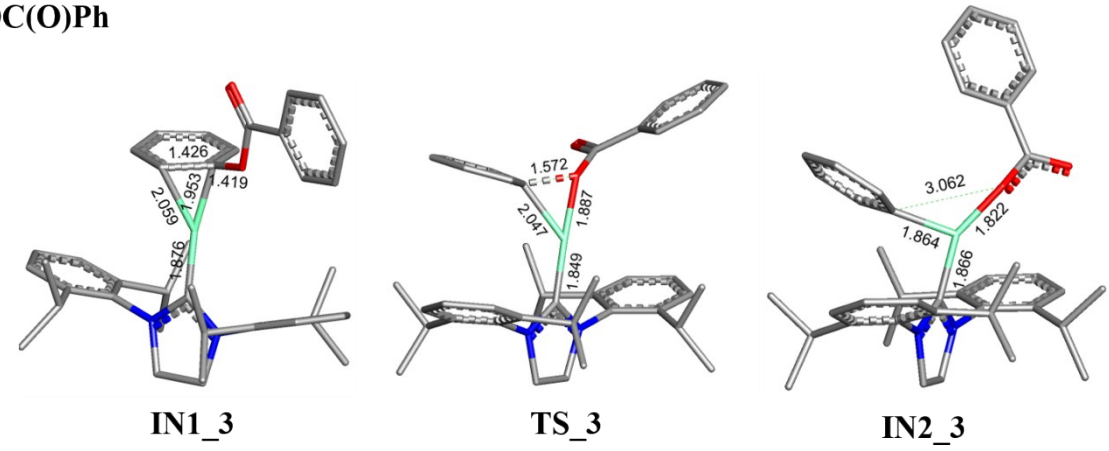

IN1_3 **TS_3** **IN2_3**

Fig. S5 Optimized structures of **IN1_3**, **TS_3**, and **IN2_3** for aryl C-O oxidative addition of phenyl esters: PhOC(O)R^2 (R^2 = ^{t}Bu, Me, and Ph). Hydrogen atoms are omitted for clarity except for those on OMe and NH_2. Bond distances are shown in Å.

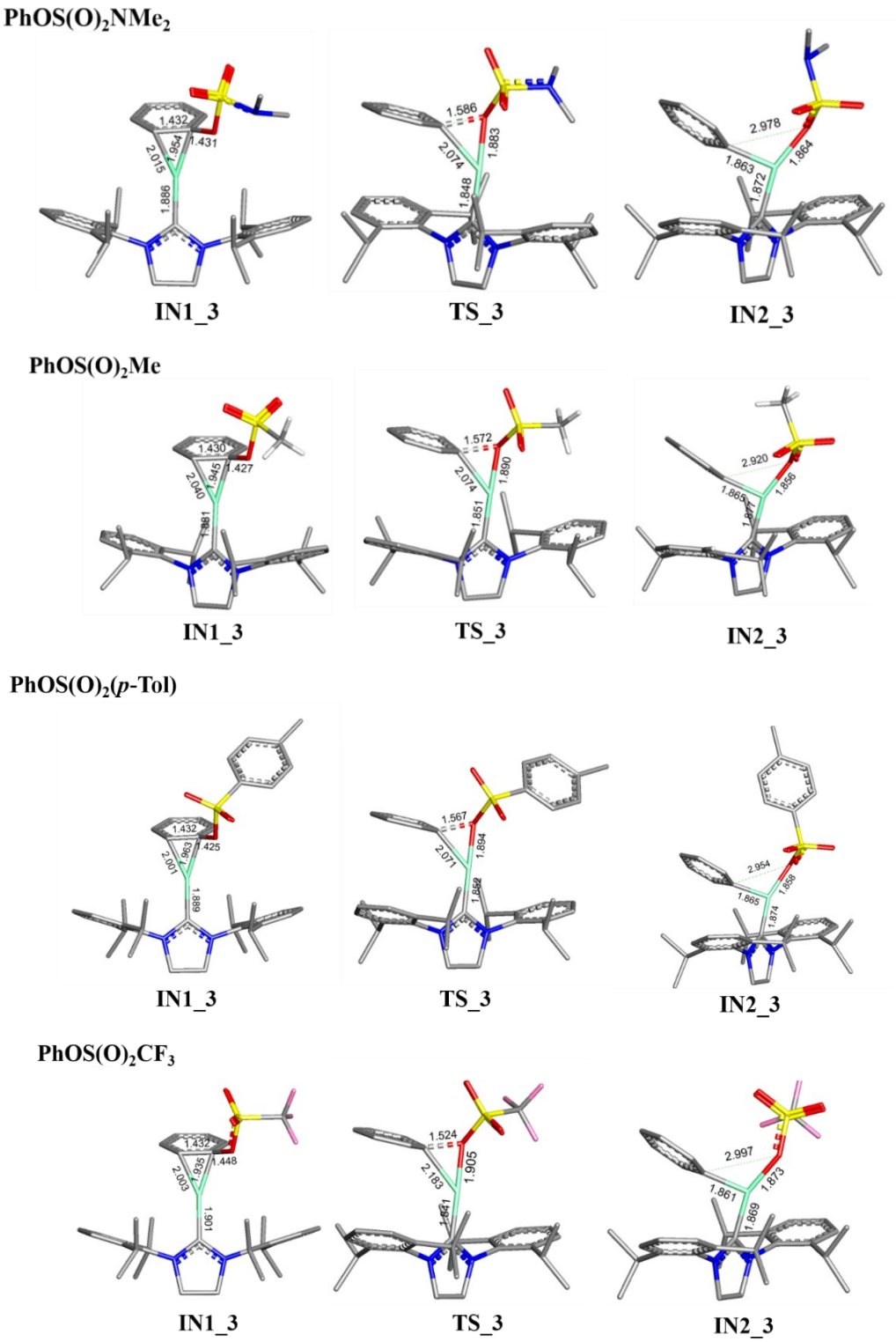

Fig. S6 Optimized structures of **IN1_3**, **TS_3**, and **IN2_3** for aryl C-O oxidative addition of phenyl sulfonates/sulfamate: $PhOS(O)_2R^3$ (R^3 = NMe_2, Me, *p*-Tol, and CF_3). Hydrogen atoms are omitted for clarity except for those on Me of $PhOS(O)_2Me$. Bond distances are shown in Å.

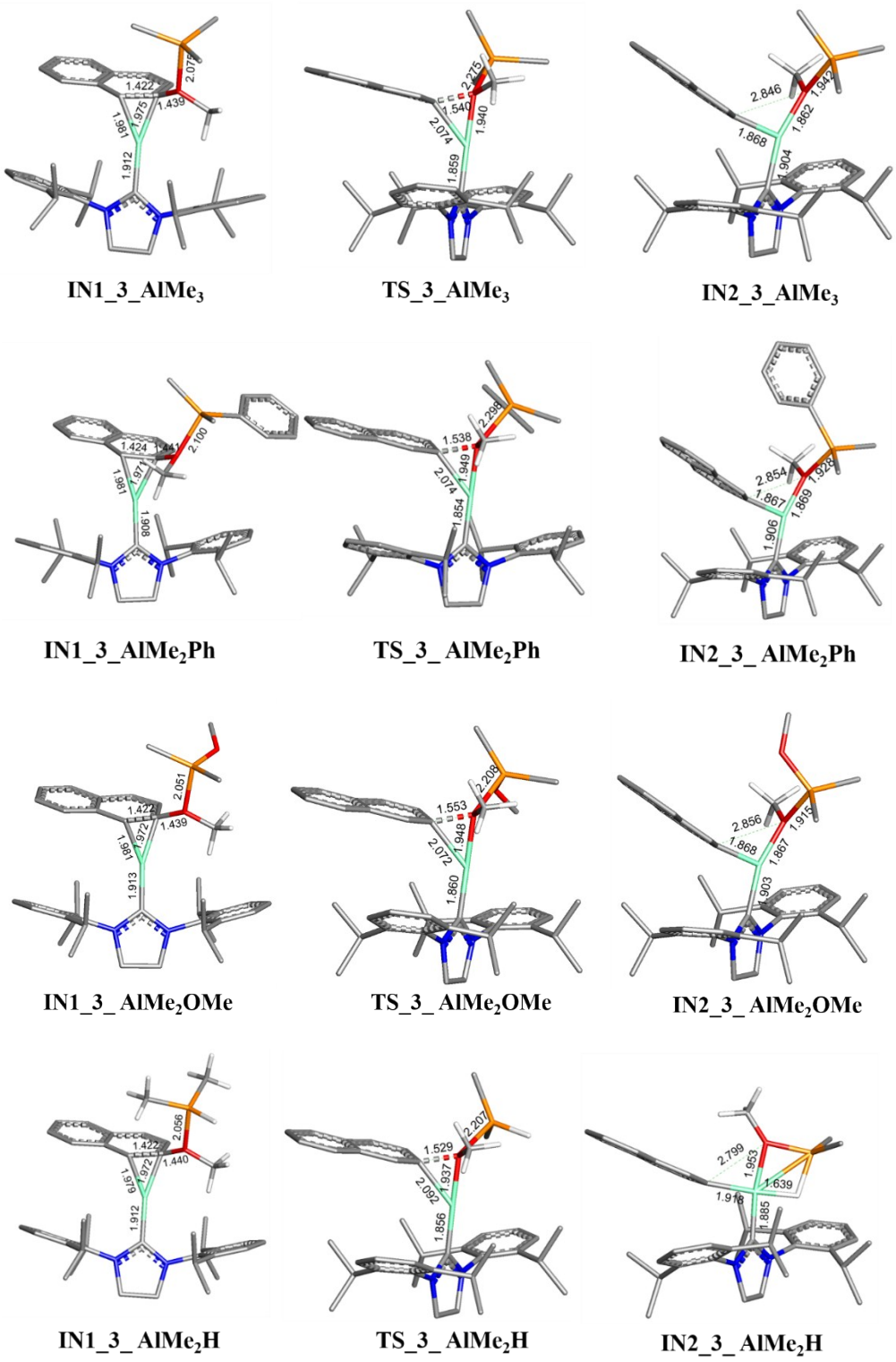

Fig. S7 Optimized structures of **IN1_3_LA**, **TS_3_LA**, and **IN2_3_LA** (LA = $AlMe_2R$; R = Me, Ph, OMe, and H) for aryl C-O oxidative addition of NaphOMe with assistance of $AlMe_3$, $AlMe_2Ph$, $AlMe_2OMe$, and $AlMe_2H$. Hydrogen atoms are omitted for clarity except for those on OMe and H of $AlMe_2H$. Bond distances are shown in Å.

PhOC(O)NEt$_2$

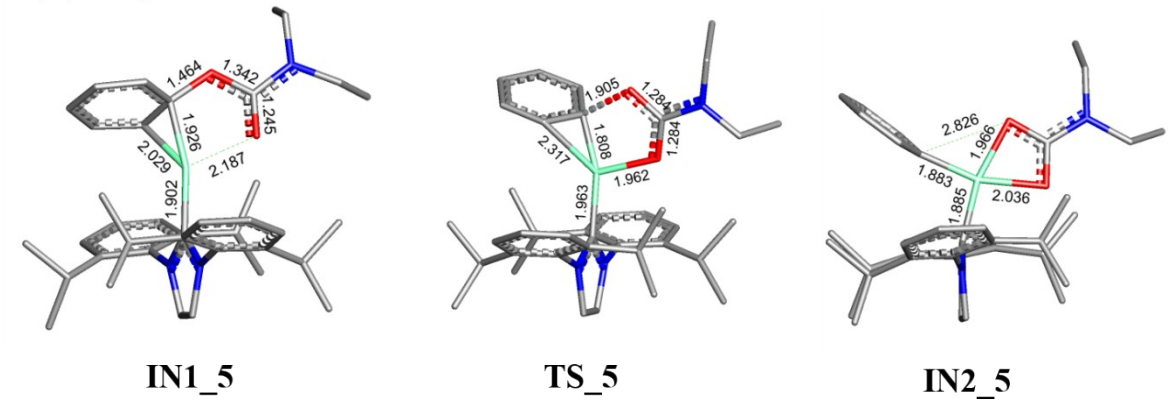

IN1_5 **TS_5** **IN2_5**

PhOC(O)NH$_2$

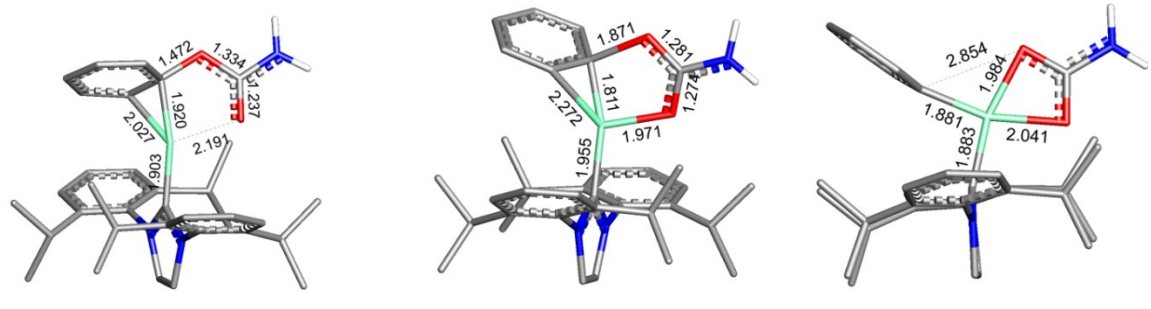

IN1_5 **TS_5** **IN2_5**

Fig. S8 Optimized structures of **IN1_5**, **TS_5**, and **IN2_5** for aryl C-O oxidative addition of phenyl carbamates: PhOC(O)R^2 (R^2 = NEt$_2$, and NH$_2$). Hydrogen atoms are omitted for clarity except for those on NH$_2$. Bond distances are shown in Å.

PhOC(O)^{t}Bu

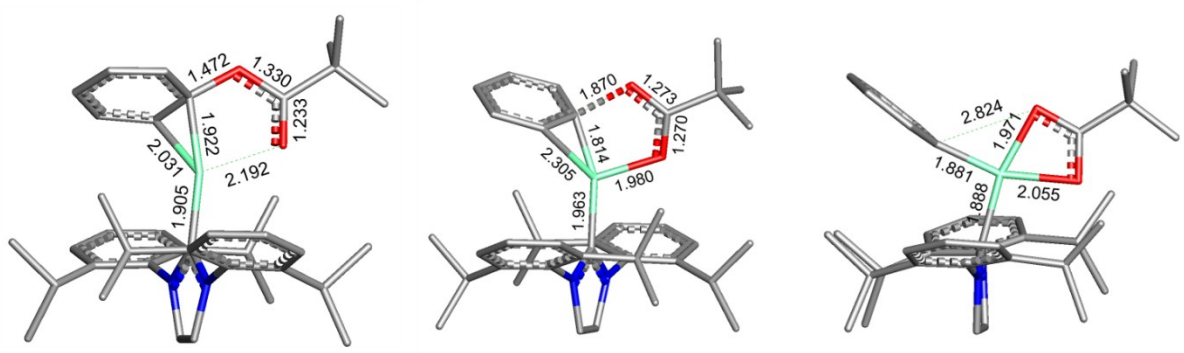

IN1_5 **TS_5** **IN2_5**

PhOC(O)Me

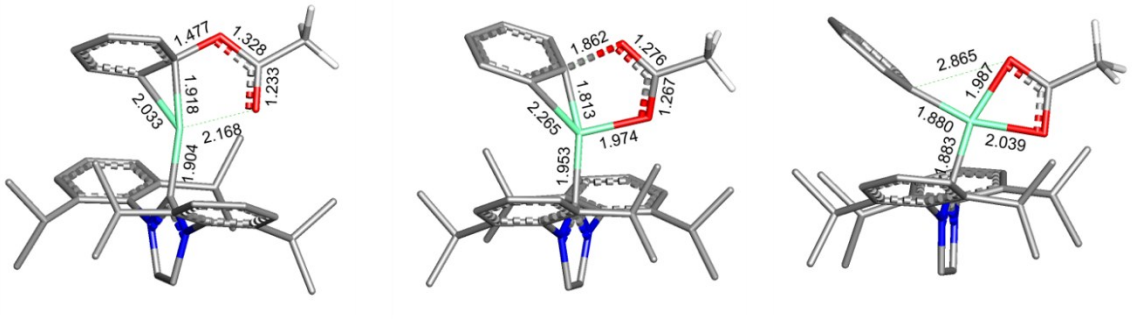

IN1_5 **TS_5** **IN2_5**

PhOC(O)Ph

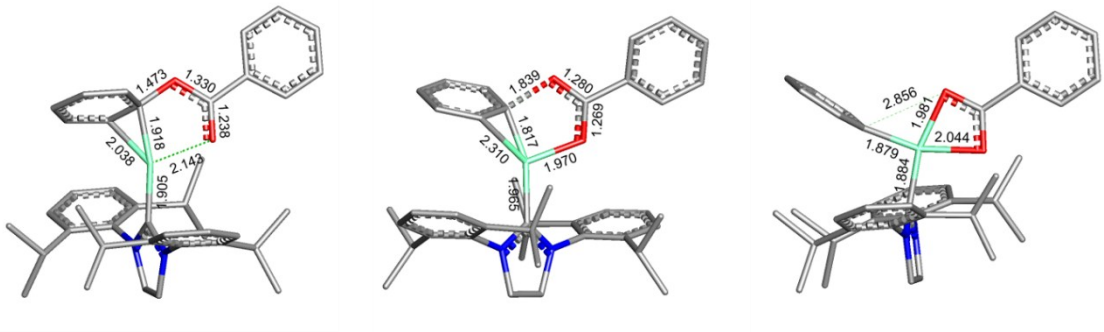

IN1_5 **TS_5** **IN2_5**

Fig. S9 Optimized structures of **IN1_5**, **TS_5**, and **IN2_5** for aryl C-O oxidative addition of phenyl esters: PhOC(O)R^2 (R^2 = ^{t}Bu, Me, and Ph). Hydrogen atoms are omitted for clarity except for those on Me of PhOC(O)Me. Bond distances are shown in Å.

PhOS(O)$_2$Me

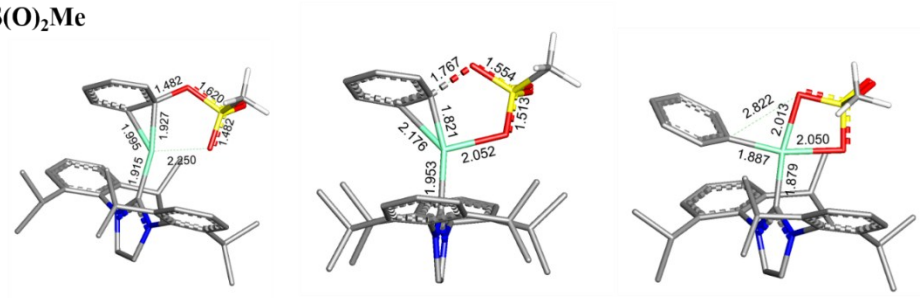

IN1_5 **TS_5** **IN2_5**

PhOS(O)$_2$(*p*-Tol)

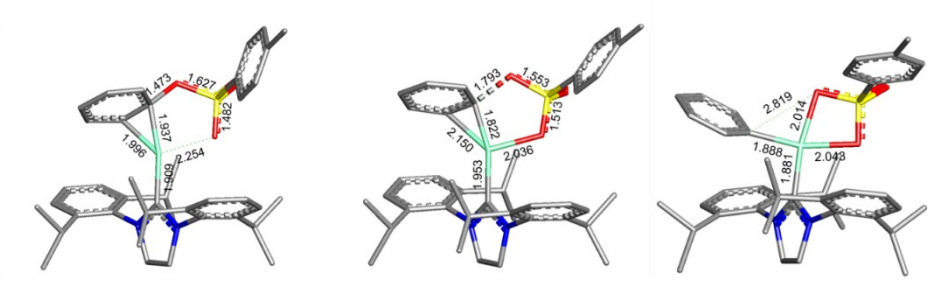

IN1_5 **TS_5** **IN2_5**

PhOS(O)$_2$CF$_3$

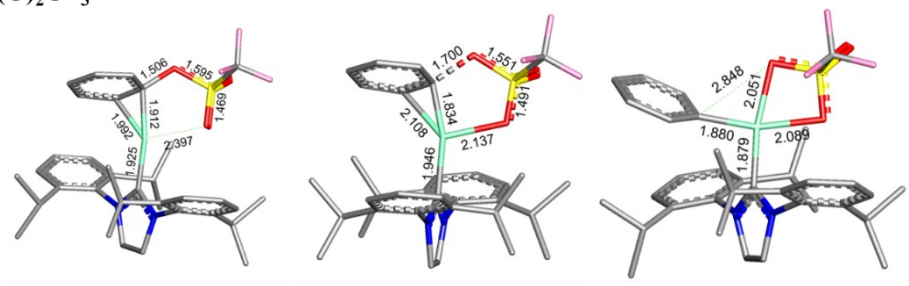

IN1_5 **TS_5** **IN2_5**

Fig. S10 Optimized structures of **IN1_5**, **TS_5**, and **IN2_5** for aryl C-O oxidative addition of phenyl sulfonates/sulfamate: PhOS(O)$_2$R^3 (R^3 = Me, *p*-Tol, and CF$_3$). Hydrogen atoms are omitted for clarity except for those on Me of PhOS(O)$_2$Me. Bond distances are shown in Å.

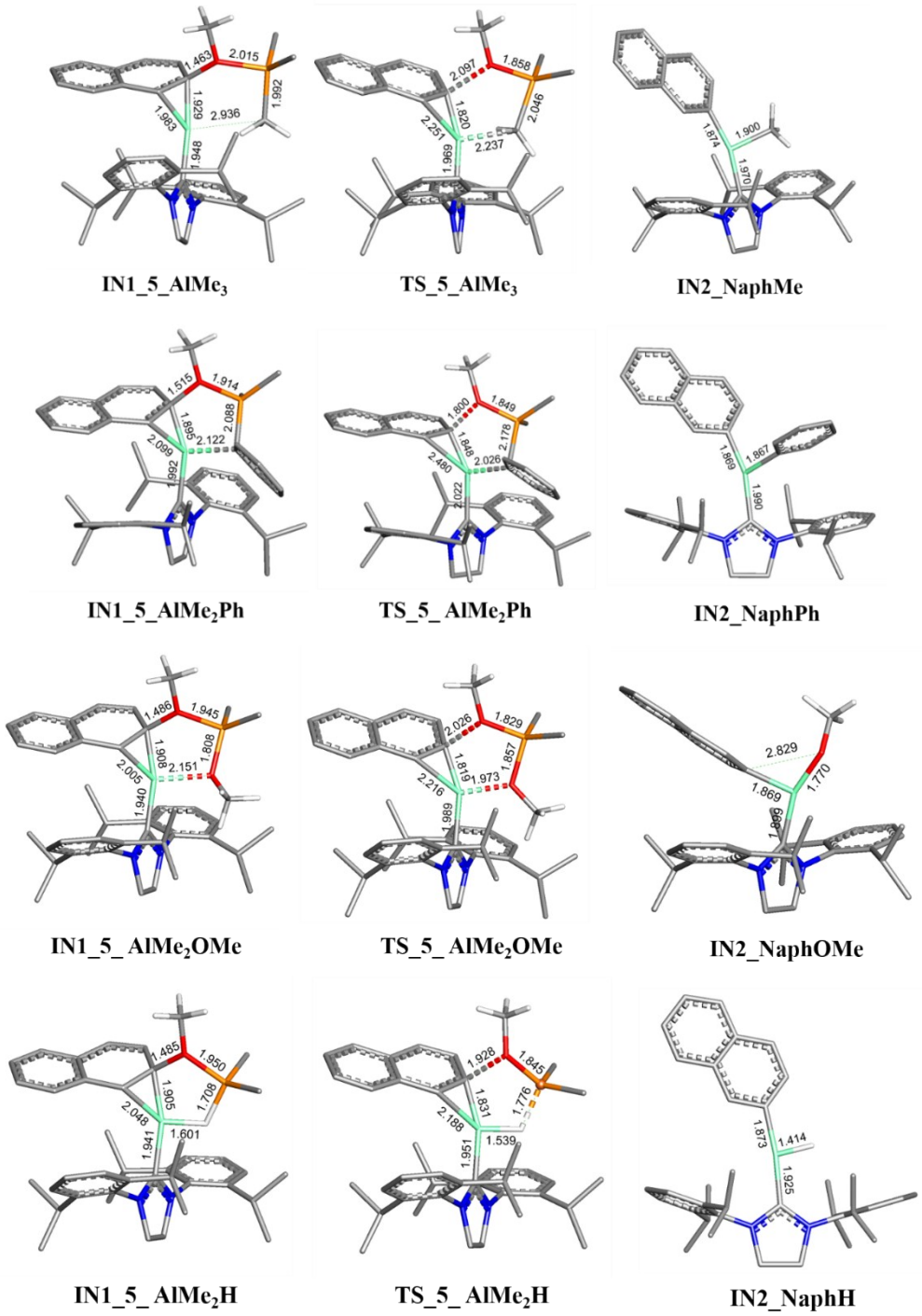

Fig. S11 Optimized structures of **IN1_5_LA**, **TS_5_LA**, and **IN2_NaphR** (LA = $AlMe_2R$; R = Me, Ph, OMe, and H) for aryl C-O oxidative addition of NaphOMe with assistance of $AlMe_3$, $AlMe_2Ph$, $AlMe_2OMe$, and $AlMe_2H$. Hydrogen atoms are omitted for clarity except for migrating Me, H and OMe of $AlMe_2R$ and OMe of NaphOMe. Bond distances are shown in Å.

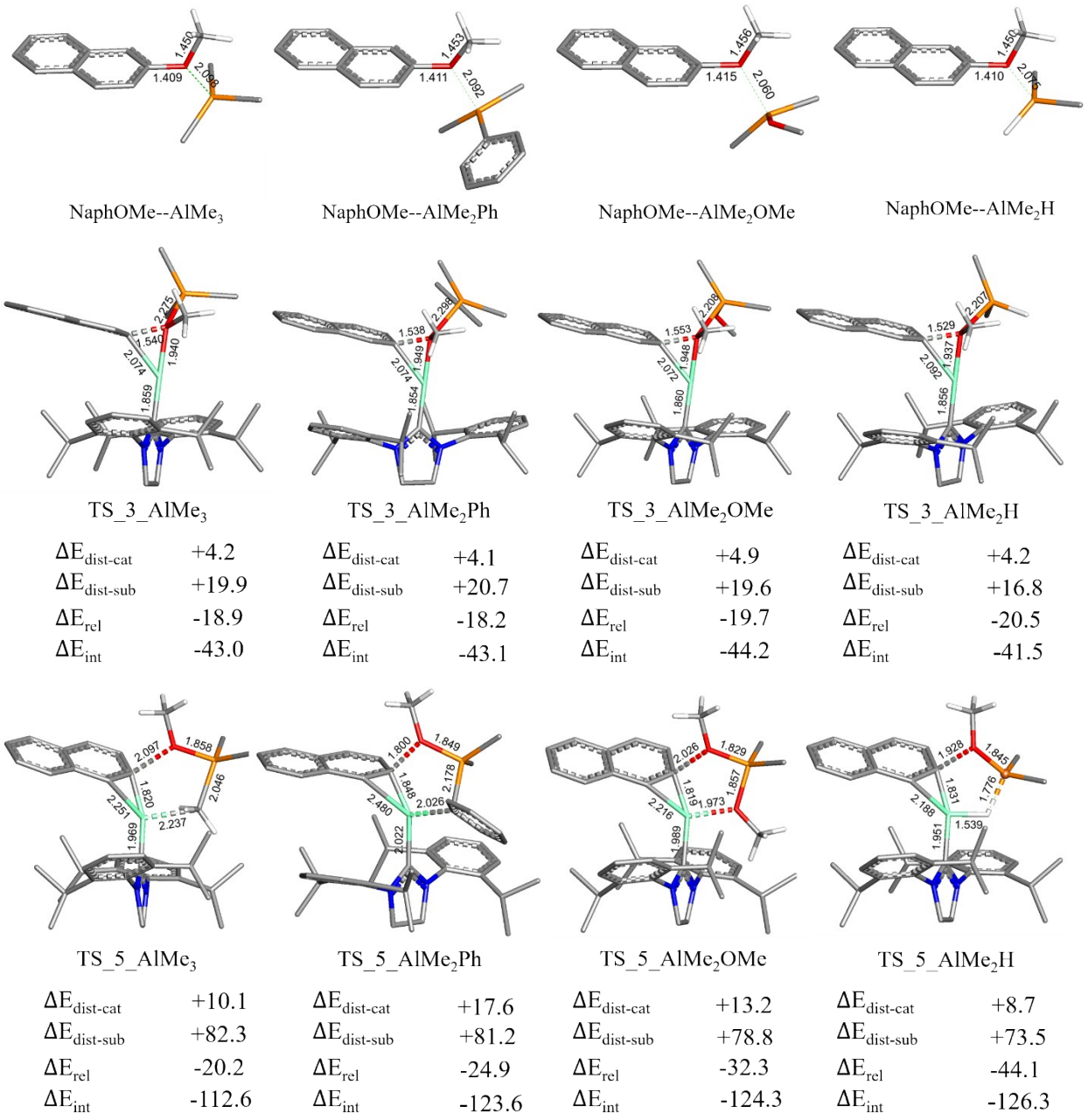

Fig. S12 Optimized geometries and distortion-interaction decomposition energies (in kcal/mol) of three-centered transition state (**TS_3_LA**) and five-centered transition state (**TS_5_LA**) (LA = $AlMe_2R$; R = Me, Ph, OMe, and H) for aryl C-O oxidative addition of NaphOMe assisted by $AlMe_2R$ Lewis acid (LA). Calculated bond distances are shown in Å. All hydrogen atoms are omitted for clarity except for those on migrating Me, H and OMe of $AlMe_2R$ and OMe of NaphOMe. Ni is shown in green, N in blue, C in grey, O in red, and H in white.

NaphOMe (B3LYP/BS1)

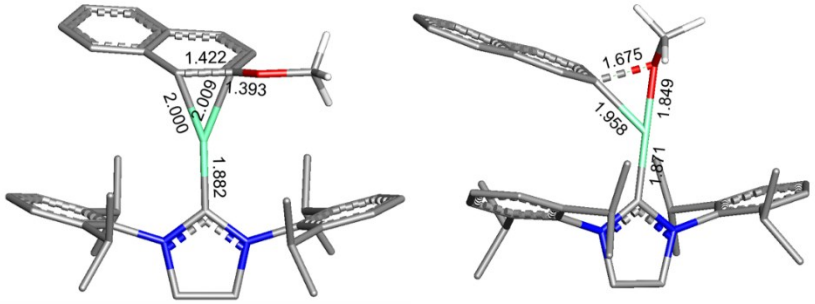

IN1_3 **TS_3**

NaphOMe (CPCM-B3LYP/BS1)

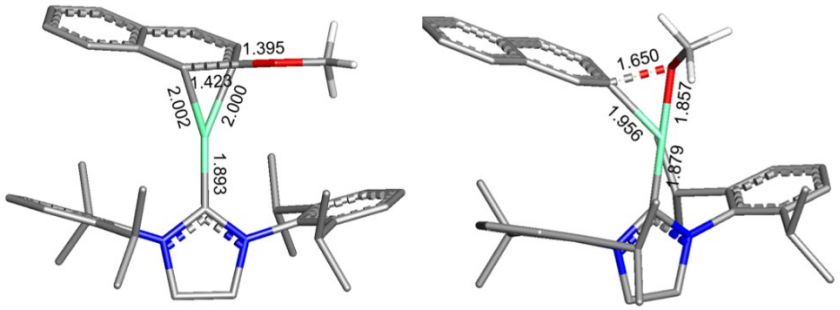

IN1_3 **TS_3**

Fig. S13 Optimized structures of **IN1_3** and **TS_3** for aryl C-O oxidative addition of NaphOMe using B3LYP/BS1 in gas phase and in solution phase.

NaphOMe (B3LYP/BS1)

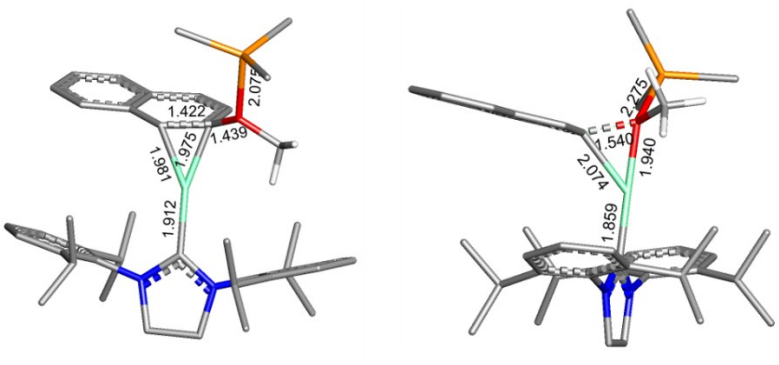

IN1_3_AlMe$_3$ **TS_3_AlMe$_3$**

NaphOMe (CPCM-B3LYP/BS1)

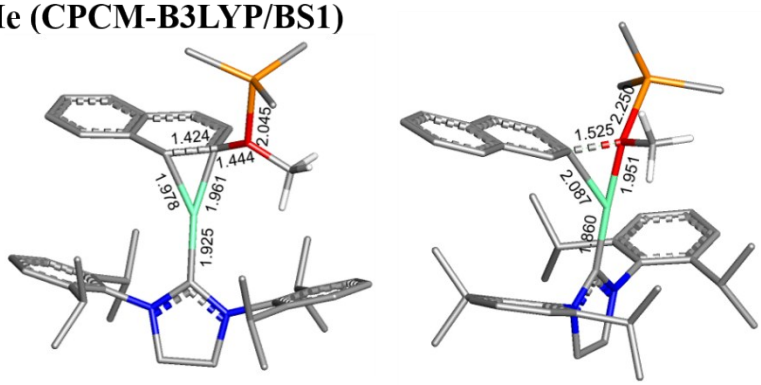

IN1_3_AlMe$_3$ **TS_3_AlMe$_3$**

Fig. S14 Optimized structures of **IN1_3_AlMe$_3$** and **TS_3_AlMe$_3$** for aryl C-O oxidative addition of NaphOMe with assistance of $AlMe_3$ using B3LYP/BS1 in gas phase and in solution phase.

NaphOMe (B3LYP/BS1)

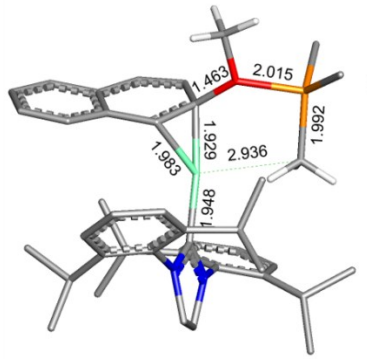

IN1_5_AlMe$_3$

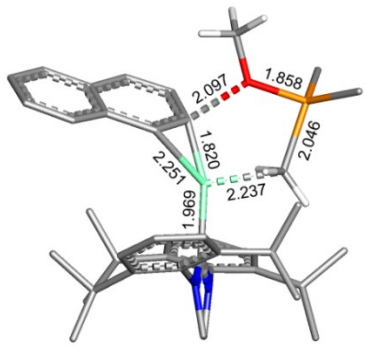

TS_5_AlMe$_3$

NaphOMe (CPCM-B3LYP/BS1)

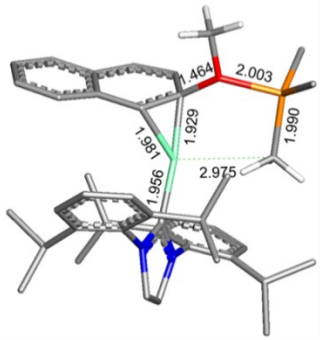

IN1_5_AlMe$_3$

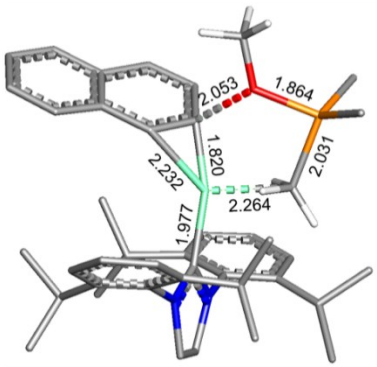

TS_5_AlMe$_3$

Fig. S15 Optimized structures of **IN1_5_AlMe$_3$** and **TS_5_AlMe$_3$** for aryl C-O oxidative addition of NaphOMe with assistance of $AlMe_3$ using B3LYP/BS1 in gas phase and in solution phase.

NaphOMe (B3LYP/BS1)

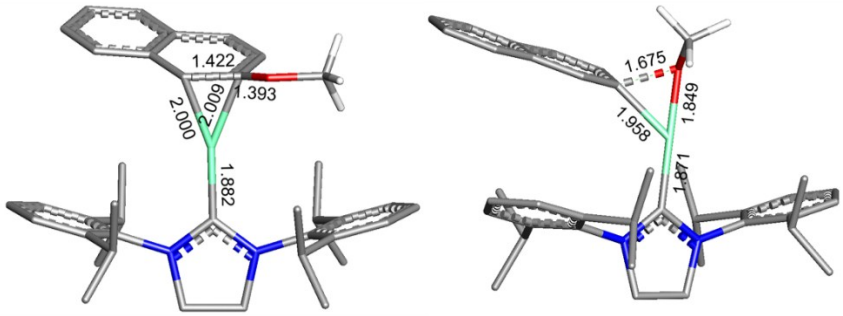

IN1_3 **TS_3**

NaphOMe (wB97XD/BS1)

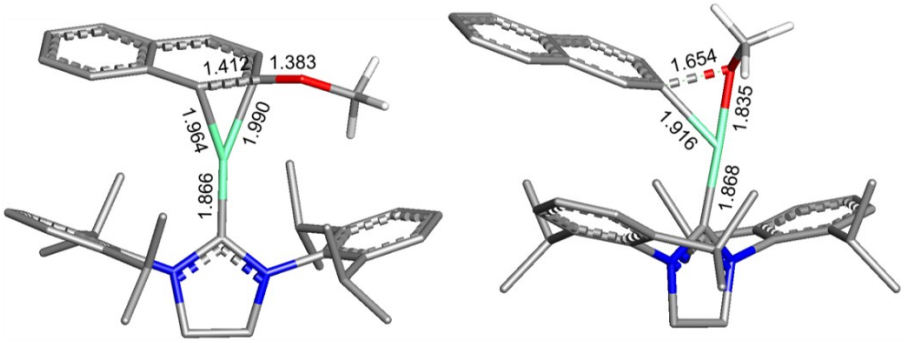

IN1_3 **TS_3**

NaphOMe (M06L/BS1)

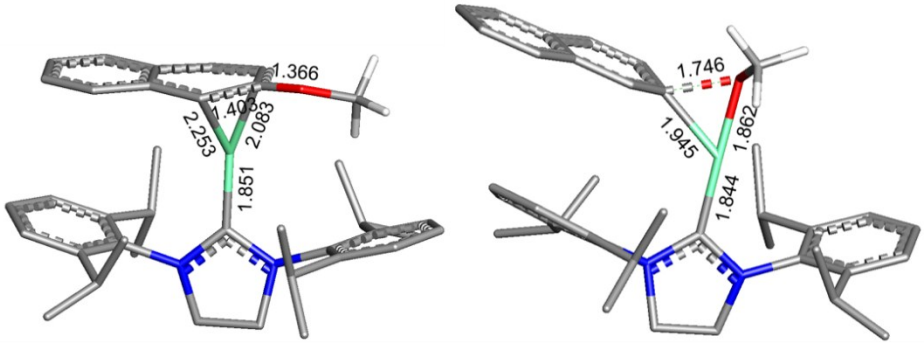

IN1_3 **TS_3**

Fig. S16 Optimized structures of **IN1_3** and **TS_3** for aryl C-O oxidative addition of NaphOMe using B3LYP, wB97XD, and M06L.

NaphOMe (B3LYP/BS1)

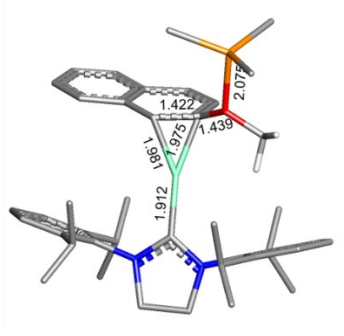

IN1_3_AlMe$_3$

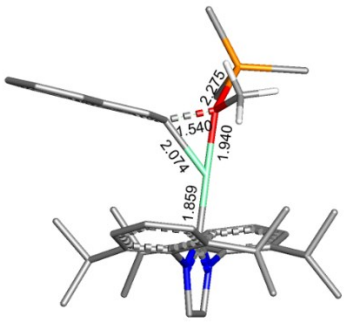

TS_3_AlMe$_3$

NaphOMe (wB97XD/BS1)

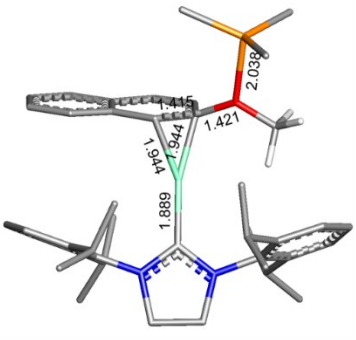

IN1_3_AlMe$_3$

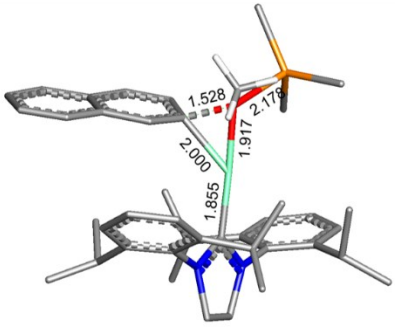

TS_3_AlMe$_3$

NaphOMe (M06L/BS1)

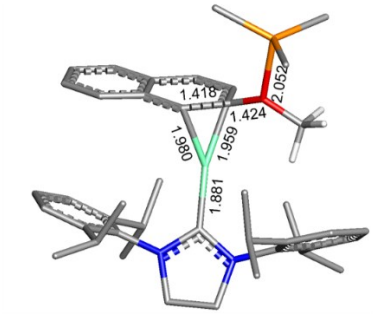

IN1_3_AlMe$_3$

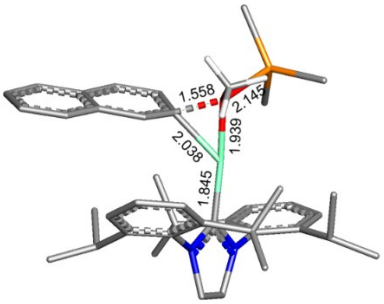

TS_3_AlMe$_3$

Fig. S17 Optimized structures of **IN1_3_AlMe$_3$** and **TS_3_AlMe$_3$** for aryl C-O oxidative addition of NaphOMe with assistance of $AlMe_3$ using B3LYP, wB97XD, and M06L.

NaphOMe (B3LYP/BS1)

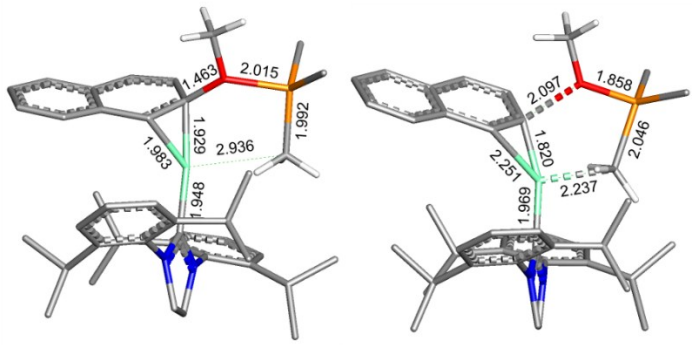

IN1_5_AlMe$_3$ **TS_5_AlMe$_3$**

NaphOMe (wB97XD/BS1)

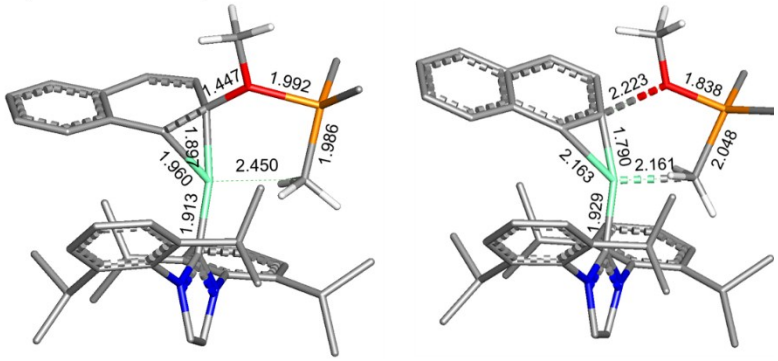

IN1_5_AlMe$_3$ **TS_5_AlMe$_3$**

NaphOMe (M06L/BS1)

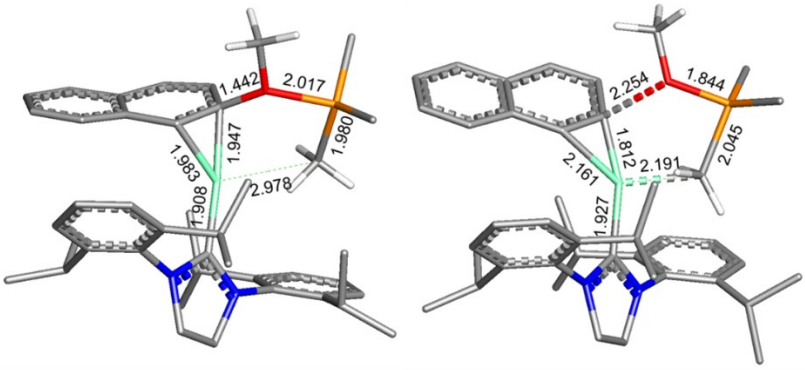

IN1_5_AlMe$_3$ **TS_5_AlMe$_3$**

Fig. S18 Optimized structures of **IN1_3_AlMe$_3$** and **TS_3_AlMe$_3$** for aryl C-O oxidative addition of NaphOMe with assistance of $AlMe_3$ using B3LYP, wB97XD, and M06L.

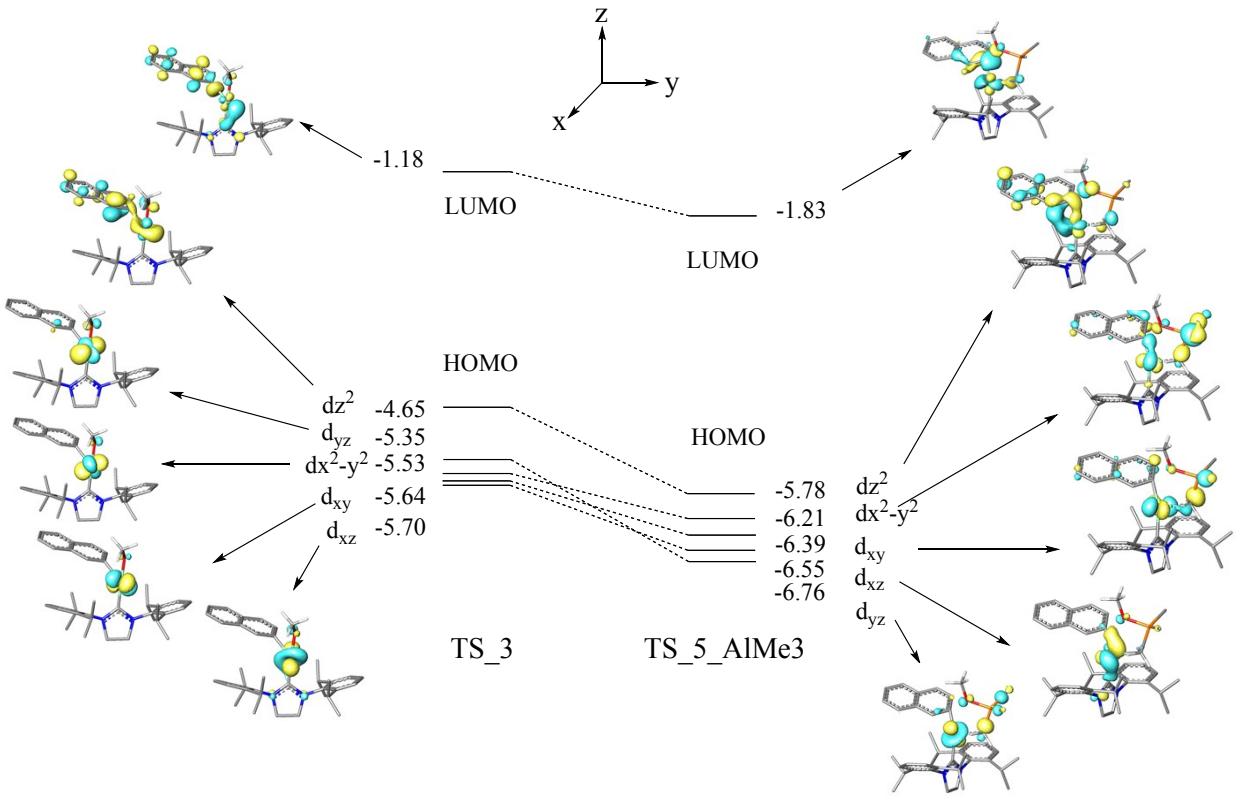

Fig. S19 Selected molecular orbitals and energies of molecular orbitals (in eV) of **TS_3** and **TS_5_AlMe$_3$** for NaphOMe.

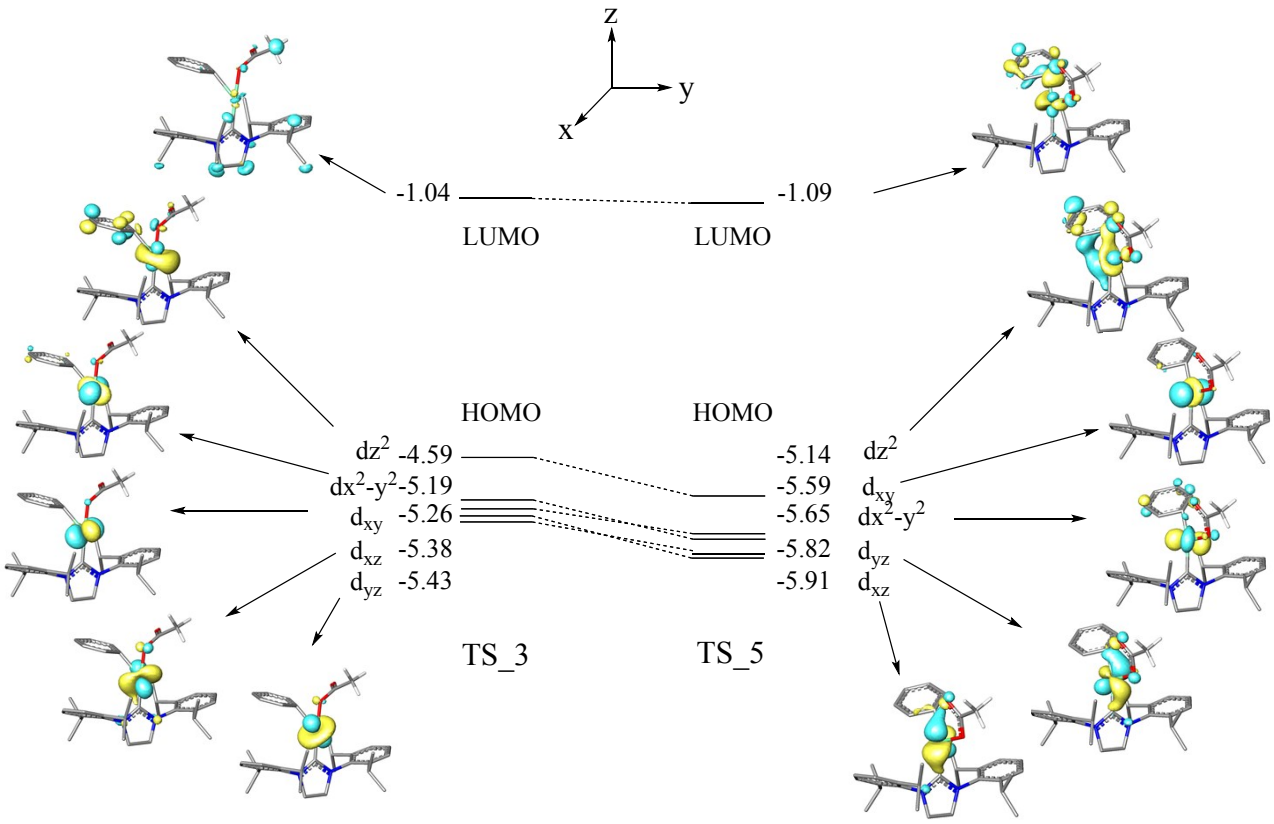

Fig. S20 Selected molecular orbitals (MOs) and MO energies (in eV) of **TS_3** and **TS_5** for PhOC(O)Me.

References

1. X. Hong, Y. Liang and K. N. Houk, *J. Am. Chem. Soc.*, 2014, **136**, 2017-2025.
2. D. H. Ess and K. N. Houk, *J. Am. Chem. Soc.*, 2007, **129**, 10646-10647.
3. F. Israel and B. F. Matthias, *J. Comput. Chem.*, 2012, **33**, 509-516.
4. F. M. Bickelhaupt and K. N. Houk, *Angew. Chem., Int. Ed.*, 2017, **56**, 10070-10086.
5. I. Fernandez and F. M. Bickelhaupt, *Chem. Soc. Rev.*, 2014, **43**, 4953-4967.
6. K. Morokuma, *J. Chem. Phys.*, 1971, **55**, 1236-1244.
7. K. Kitaura and K. Morokuma, *Int. J. Quantum Chem.*, 1976, **10**, 325-340.